

A New Multi-objective Microgrid Restoration Via Semidefinite Programming

Liang Zhao*, Wen-Zhan Song*

* Department of Computer Science, Georgia State University
Atlanta, GA USA. Email: lzhao5@student.gsu.edu, wsong@gsu.edu

Abstract—This paper presents a new multi-objective microgrid reconfiguration problem formulation. Unlike existing distribution system or microgrid reconfiguration algorithms, we consider the effect of uncertainty arising from the renewable energy generation and investigate the tradeoff between the invented index measuring the reliability of reconfiguration and the total load served. The resulting optimization problem is computationally prohibitive due to the binary circuit breaker variables and the probability constraint accounting for the uncertainty of renewable generation. Nevertheless, a semidefinite programming (SDP) reformulation is developed based on convex relaxation techniques and the scenario-based approximation. Furthermore, weighted-sum method is applied in the reformulation and we eventually obtain the Pareto solution points of the microgrid reconfiguration. Numerical tests validate the intrinsic tradeoff between the two objectives and demonstrate the effectiveness of the proposed solution methodology.

Keywords—Microgrid, Multi-Objective optimization, Convex relaxation, Semidefinite Programming, Weighted-Sum Method.

I. INTRODUCTION

The evolving next generation power grid, so-named Smart Grid has attracted considerable attention in academic and industry communities. As an important content of smart grid, the concept of smart microgrid has been proposed recently. Unlike traditional power grid, microgrid has three important features. First, it owns a small-scale group of generation resources and local customers itself. Second, microgrid is able to manage its energy system in a cooperative fashion based on two-way communications and bidirectional electricity paths. Third, microgrid is a promising way to integrate distributed generations (DGs) (i.e., renewable energy resources (RES)) on the local community in order to diversify energy supply and improve efficiency [1].

Microgrids belong to an area where the cyber and physical worlds meet. It is an application of the Cyber-Physical System (CPS) in which sensing, networking, and computing are tightly coupled with the control of the physical power grid. In the cyber-layer, one of the challenges is distributed resource management. Fortunately, the advances in information infrastructure such as “smart sensors” provide opportunities to better cope with this issue [2]. Based on the collected information on loads, generators and transmission lines, etc., system operator can have the potential of continuous decision-making and monitoring over the grid.

Although smart grid has been featured by a series of important functionalities, the capability of self-reconfiguration

takes a leading role [3]. The self-reconfiguration enables smart grids to redirect their power flows in an appropriate way, e.g., via changing topologies, shedding loads, and other control measures, to achieve certain desirable objectives. Considering the great penetration of RES in smart microgrids, the self-reconfiguration of smart microgrids needs a careful design to address the volatility in the RES generations [4], [5].

II. RELATED WORK

At present, a lot of research efforts have been conducted on conventional distribution system and microgrid reconfiguration. In [6], [7], [8], [9], minimizing the active power loss (or total power loss) was considered as the sole objective. Multi-objective formulation of the reconfiguration problem was investigated in [10]. Besides the objective of minimization of the total power loss, [10] also considers minimizing both the nodes voltage deviation and the violation of line current limit. Consequently, it is a more advanced and realistic formulation comparing to the single-objective ones. However, in case of an emergency, power accessibility is a more important issue than economical reasons. Thus, the main goal in such scenarios should be to serve as much critical total loads as possible in the system. Recent work of reconfiguration for quick service restoration in distribution systems or microgrids were discussed in [11], [12], [13]. However, like all the aforementioned frameworks, they are not suitable for microgrids since the presence of RES is not considered, which is an important feature of future smart microgrids.

Motivation of using SDP: The ideal Pareto front is usually not known. Therefore, the Pareto solution set generated by any algorithm is considered as an estimate of the ideal Pareto set. Most multi-objective formulations are based on evolutionary algorithms [10], [14], which are population-based and can generate the Pareto front estimate in a single run. Due to the stochastic nature of evolutionary algorithms, the attainment of the ideal Pareto front may be difficult or even impossible. In comparison, the SDP-based weighted sum is not a population-based algorithm. It is convex and will provide globally optimum Pareto solutions when the relaxation is tight.

Considering all the issues above, we are thus motivated to design a new microgrid restoration framework through SDP. The main contributions of this paper can be summarized as follows.

- A novel multi-objective microgrid reconfiguration problem formulation is proposed in which we consider both

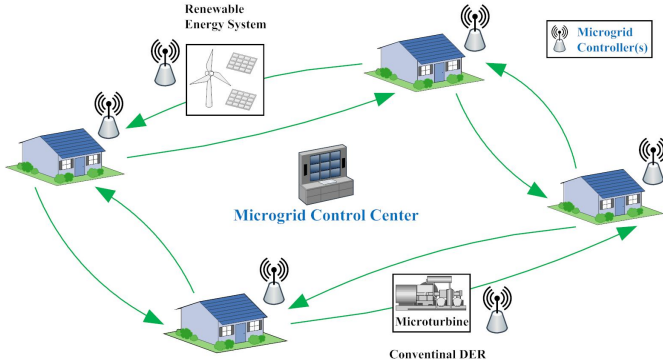


Fig. 1. An example microgrid CPS required for self-reconfiguration.

the objectives of total loads served and a new index measuring the reliability of reconfiguration operation.

- Since the volatility of RES generations has not been considered in existing reconfiguration algorithms, this paper proposes an extended formulation containing the constraint for such volatility.
- The resultant optimization problem is computationally prohibitive. Nevertheless, a convex semidefinite programming (SDP) reformulation is developed, which outperforms NSGA-II in several respects.

We organize the rest of this paper in the following way. The system architecture and the multi-objective problem formulation are described in Section III. Next in Section IV, we present the derivation of the computationally tractable reformulation of the microgrid reconfiguration problem. Section V focuses on the conversion of the reformulated multi-objective problem into its scalar equivalent via the weighted-sum method. In Section VI, the effectiveness of the proposed approach is evaluated. Section VII provides the conclusion and final remarks.

III. SYSTEM ARCHITECTURE AND PROBLEM STATEMENT

A. System Architecture

Fig. 1 depicts the system architecture for the microgrid reconfiguration. The houses can be residential households or other consumers (i.e., hospitals). The green arrows are bidirectional energy paths between two neighboring units. There are conventional DERs and renewable energy for the power supply. More importantly, microgrid “controllers” (e.g. various smart sensors) are installed in the physical units across the grid. For example, the microgrid control center can adjust the wind turbine based on the wind profile (captured by its controller) to achieve higher efficiency. In short, the control center can perform grid resource management (such as grid reconfiguration, load balancing) based on the timely information provided by this cyber system.

B. Problem Description

We consider a microgrid as a graph in this paper. The vertices represent the buses in the power grid. Each bus has load and generation units (i.e., conventional distributed

generation units and renewable energy generators). The set of edges denotes the branches in the microgrid. It is assumed that all branches have circuit breakers. The load in each bus is also assumed to have circuit breaker attached modeling the possible action of load shedding. The loads in the system have different priorities. This means that some loads (i.e., medical services) are more critical than others (i.e., residential households). Our reconfiguration scheme is expected to guarantee these critical loads served first. The reconfiguration is modeled as a decision problem simultaneously maximizing the loads served and the operation reliability. Relevant notations are listed in TABLE I.

TABLE I
NOTATIONS

P_{G_i}	conventional DG units power generation on i -th bus.
P_{R_i}	RES power generation on i -th bus (random variable).
P_{L_i}	actual power consumption on i -th bus.
$P_{t_{ij}}$	power flow between i -th bus and j -th bus.
S_{L_i}	circuit breaker status at the load of i -th bus.
λ_{M_i}	weighting factor for the load of i -th bus.
N	the set of buses in the microgrid.
B	the set of branches in the microgrid.
N_i	the set of neighboring buses to i -th bus.
c_{ij}	the power flow limit in branch (i, j) .
$P_{G_i}^{min}$	minimum amount of DG units power generation on i -th bus.
$P_{G_i}^{max}$	maximum amount of DG units power generation on i -th bus.
$P_{L_i}^{min}$	minimum required actual power consumption on i -th bus.
$P_{L_i}^{max}$	maximum actual power consumption on i -th bus.

C. Objectives in the Problem Formulation

We first describe the two different objectives adopted in the presenting paper.

1) *Total Loads Served*: We consider the microgrid reconfiguration for service restoration. It is usually taken place after the fault occurrence. Hence an important goal is to restore the power supply service to the loads in the system [9], [12]. Specifically, the objective of total loads served can be expressed as:

$$\sum_{i=1}^{|N|} \lambda_{M_i} S_{L_i} P_{L_i} \quad (1)$$

where the parameter λ_{M_i} accounts for the priority of load i . Specifically, in objective (1), the set of λ_{M_i} helps put the loads with high priority to be supplied first.

2) *Reliability of Reconfiguration Operation*: In the reconfiguration process, it is reasonable and meaningful to take the operating reliability into account since it is highly required to avoid service interruption again in a short period. We define the

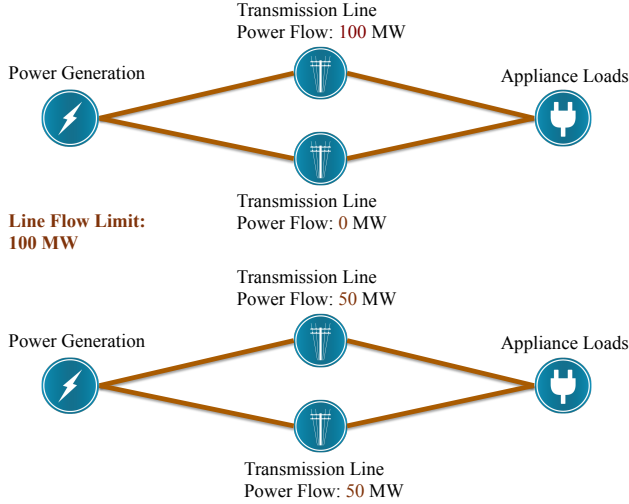


Fig. 2. Illustration of measuring the reliability of reconfiguration operation under two different cases. The power generation source needs to supply 100 MW to the appliance loads and there are two transmission lines between them. The upper case solution has reliability value 0 MW while the bottom one has reliability value 50 MW based on the definition in (2). It is stated that the upper one is more vulnerable than the bottom one since one of the lines in upper case is reaching the line flow limit.

reliability of reconfiguration operation using the mathematical expression as follows.

$$\min_{(i,j) \in B} \{c_{ij} - |P_{t_{ij}}|\} \quad (2)$$

Equation (2) is to first compute the distance of actual power flow to its limit for each branch, and find the minimum distance among them. This measure is important since operating power flow close to its limit will greatly increase the probability of failure and be more vulnerable to contingencies. A simple example in Fig. 2 shows cases with different values of operation reliability.

D. Uncertainty in Renewable Energy Generation

Another distinct assumption made in our reconfiguration problem is that renewable energy generators are involved in supplying power to the grid. They are considered to be widely used and installed in each bus. Unfortunately, the energy output of renewable generators (denoted as random variables P_{R_i} in this paper) will fluctuate around its forecasted values due to e.g., fast-varying weather conditions [4], [5]. Thus, at some time, the power supply available at some buses might not satisfy their power required. As a result, it is essential to perform a grid reconfiguration that is capable of limiting this kind of risk.

E. Microgrid Reconfiguration Formulation

Based on the system model described above, we formulate the microgrid reconfiguration as the optimization problem (P1)

as follows.

$$\begin{aligned} \text{(P1)} \quad & \max_{\mathcal{V}} \left[\sum_{i=1}^{|N|} \lambda_{M_i} S_{l_i} P_{L_i}, \min_{(i,j) \in B} \{c_{ij} - |P_{t_{ij}}|\} \right]^T \quad (3a) \\ \text{s.t.} \quad & -c_{ij} \leq P_{t_{ij}} \leq c_{ij}, (i,j) \in B \quad (3b) \\ & -S_{t_{ij}} \times c_{ij} \leq P_{t_{ij}} \leq S_{t_{ij}} \times c_{ij}, (i,j) \in B \quad (3c) \\ & P_{G_i}^{min} \leq P_{G_i} \leq P_{G_i}^{max}, \forall i \in N \quad (3d) \\ & S_{l_i} \times P_{L_i}^{min} \leq P_{L_i} \leq S_{l_i} \times P_{L_i}^{max}, \forall i \in N \quad (3e) \\ & S_{l_i} \in \{0, 1\}, \forall i \in N \quad (3f) \\ & S_{t_{ij}} \in \{0, 1\}, (i,j) \in B \quad (3g) \\ & \Pr \left(P_{G_i} + P_{R_i} - \sum_{j \in N_i} P_{t_{ij}} \geq P_{L_i}, \forall i \in N \right) \geq 1 - \epsilon \quad (3h) \end{aligned}$$

where $\mathcal{V} := \{P_{G_i}, P_{L_i}, P_{t_{ij}}, S_{l_i}, S_{t_{ij}}\}$ contains all the decision variables. Specifically, the objective function (3a) takes accounts of two different aspects, namely, the total power served and the index of operational reliability; Constraint (3b) illustrates that the power flow along the lines should conform with their line limits; Constraint (3c) ensures that the power will flow through the bus pair (i, j) only when the breaker on this branch is closed; Constraint (3d) represents the generator capacity in each bus; Constraint (3e) models the possible action of load curtailment by the system operator. Furthermore, constraints (3f) and (3g) represent the binary state of circuit breakers in the buses (for the loads) and the branches respectively; Finally, constraint (3h) requires that the actual power supply at each bus satisfies its demand with probability no less than $1 - \epsilon$, where ϵ is a pre-selected threshold.

Unfortunately, solving (P1) is computationally difficult for the following reasons:

- r1:** The bilinear term $S_{l_i} P_{L_i}$ in (3a) renders (P1) non-convex, which implies that (P1) is difficult to solve optimally and efficiently in general;
- r2:** Due to the binary variables $\{S_{l_i}, S_{t_{ij}}\}$, solving (P1) is NP-hard;
- r3:** The probabilistic constraint (3h) is generally in a computationally intractable form.

We propose an approach to cope with **r1-r3** in the ensuing section with a computationally tractable reformulation of (P1).

IV. COMPUTATIONALLY TRACTABLE REFORMULATION

We first derive an alternative problem formulation of (P1) that has linear objectives as follows.

$$\begin{aligned} \text{(P2)} \quad & \min_{\mathcal{V}'} \left[t_1, t_2 \right]^T \quad (4a) \\ \text{subject to:} \quad & (3b) - (3h) \text{ and} \quad (4b) \\ & \sum_{i=1}^{|N|} \lambda_{M_i} S_{l_i} P_{L_i} \geq -t_1 \quad (4c) \\ & -(c_{ij} + t_2) \leq P_{t_{ij}} \leq (c_{ij} + t_2), (i,j) \in B \quad (4d) \end{aligned}$$

where $\mathcal{V}' := \{P_{G_i}, P_{L_i}, P_{t_{ij}}, S_{l_i}, S_{t_{ij}}, t_1, t_2\}$ collects the reconfiguration decision variables.

A closer look into (P1) and (P2) reveals the following proposition.

Proposition 1. *The problems in (P1) and (P2) are equivalent.*

Proof. In the first place, the objective in (3a) is equivalent to the following:

$$\min \left[-\sum_{i=1}^{|N|} \lambda_{M_i} S_{l_i} P_{L_i}, -\min_{(i,j) \in B} \{c_{ij} - |P_{t_{ij}}|\} \right]^T$$

Second, we start with the trick of introducing two auxiliary variables t_1 and t_2 that serve as the upper bounds on the two objectives respectively. Thus, the above objective can be cast as (4a) with two extra constraints as follows:

$$\begin{aligned} -\sum_{i=1}^{|N|} \lambda_{M_i} S_{l_i} P_{L_i} &\leq t_1 \\ -\min_{(i,j) \in B} \{c_{ij} - |P_{t_{ij}}|\} &\leq t_2 \end{aligned}$$

Here, the first constraint is the same as (4c). The second constraint means that the minimum value of $c_{ij} - |P_{t_{ij}}|$ among all branches $(i, j) \in B$ is at least $-t_2$. In other words, every branch $(i, j) \in B$ satisfies the condition that $c_{ij} - |P_{t_{ij}}|$ is greater or equal to $-t_2$, that is $c_{ij} - |P_{t_{ij}}| \geq -t_2, (i, j) \in B$. It can become (4d) after several steps of algebraic manipulations. \square

Note that the vector optimization problem (P2) can be decomposed into two single-objective problems. The first single-objective problem in (P2) has objective function t_1 and the second problem has objective function t_2 , which are linear objectives. Besides, the two problems have the same constraints. Thus, in this section, which is dealing with difficult constraints arising from **r1-r3** of the optimization program, all the involving implicit objective functions are linear.

A. Convex Relaxation of Bilinear Inequalities (for **r1**)

Bilinear inequalities such as (4c) can be categorized into the form of so-called *Bilinear Matrix Inequalities* (BMIs). Problems involving BMIs have been a focus in mathematical programming as well as the robust control theory. Unfortunately, BMIs are known to be nonconvex constraints. They are computationally complex and hard to be solve [15]. The BMI Feasibility Problem is even shown to be NP-hard [16]. To relax this problem, one way is to search for a convex set which includes BMIs and closely approximates the BMIs. Replacing BMIs by such a set, the optimization problem becomes convex and therefore tractable [17].

To address **r1**, we adopt the convex relaxation method in [15] to approximate the non-convex set specified by the constraint in (4c).

We first define a new variable $Q_i = P_{L_i} S_{l_i}, \forall i \in N$. Then (4c) is equivalent to the following:

$$\sum_{i=1}^{|N|} \lambda_{M_i} Q_i \geq -t_1 \quad (5a)$$

$$Q_i = P_{L_i} S_{l_i}, \forall i \in N \quad (5b)$$

By applying the convex relaxation advance in [15], (5b) is replaced by:

$$Q_i \leq P_{L_i} \overline{S_{l_i}} + \overline{P_{L_i}} S_{l_i} - \overline{P_{L_i}} \overline{S_{l_i}}, \forall i \in N \quad (6a)$$

$$Q_i \leq P_{L_i} S_{l_i} + \overline{P_{L_i}} S_{l_i} - \overline{P_{L_i}} \underline{S_{l_i}}, \forall i \in N \quad (6b)$$

$$Q_i \geq P_{L_i} \underline{S_{l_i}} + \overline{P_{L_i}} S_{l_i} - \overline{P_{L_i}} \underline{S_{l_i}}, \forall i \in N \quad (6c)$$

$$Q_i \geq P_{L_i} \overline{S_{l_i}} + \overline{P_{L_i}} S_{l_i} - \overline{P_{L_i}} \overline{S_{l_i}}, \forall i \in N \quad (6d)$$

where $\underline{P_{L_i}}, \overline{P_{L_i}}$ are the minimum and maximum values of variable P_{L_i} respectively. Similarly, $\underline{S_{l_i}}, \overline{S_{l_i}}$ are the minimum and maximum values of variable S_{l_i} , which are known constants. In our problem, according to the formulation in previous, $\underline{P_{L_i}} = 0, \overline{P_{L_i}} = P_{L_i}^{max}, \underline{S_{l_i}} = 0, \overline{S_{l_i}} = 1$. Putting those facts into constraints (6a)-(6d) yields:

$$Q_i \leq P_{L_i}, \forall i \in N \quad (7a)$$

$$Q_i \leq P_{L_i}^{max} S_{l_i}, \forall i \in N \quad (7b)$$

$$Q_i \geq 0, \forall i \in N \quad (7c)$$

$$Q_i \geq P_{L_i} + P_{L_i}^{max} (S_{l_i} - 1), \forall i \in N \quad (7d)$$

Now, the constraint in (4c) containing bilinear term is replaced by (5a) and (7a)-(7d). Note that (5a) and (7a)-(7d) are linear constraints with respect to decision variables $\{Q_i, P_{L_i}, S_{l_i}\}$.

B. SDP Relaxation of 0-1 Integer Constraint (for **r2**)

Regarding the issues in **r2**, we use the semidefinite relaxation technique in [18] to obtain a convex-relaxed version of binary variable constraints in (3f) and (3g). In the following, we will present the detailed derivation of the aforementioned conversion.

1) *Background on SDP Relaxations:* In general, SDP relaxation is a subfield of convex relaxation techniques. Particularly, it has been applied to many difficult problems in combinatorial optimization, signal processing, and control theory. SDP relaxation is proven to provide a very tight bound for several classes of nonconvex problems [18].

To briefly illustrate the SDP relaxation technique, we consider the binary quadratic problem as follows.

$$\begin{aligned} &\text{minimize} \quad \mathbf{s}^T \mathbf{W} \mathbf{s} \\ &\text{subject to} \quad \mathbf{s} = \{0, 1\}^n \end{aligned} \quad (8)$$

where matrix \mathbf{W} is semidefinite. The 0-1 quadratic program is a well-known difficult optimization problem since it is shown to be equivalent to Max-Cut [19], which is in the class of NP-hard problems (many of its problem instances would be intractable).

The cost function in (8) can be rewritten as:

$$\mathbf{s}^T \mathbf{W} \mathbf{s} = \langle \mathbf{W}, \mathbf{s} \mathbf{s}^T \rangle \quad (9)$$

where $\langle \cdot \rangle$ indicates inner product operation. Following the idea of linearization, we introduce a matrix variable \mathbf{S} to take the role of \mathbf{ss}^T . The binary constraint in (8) is equivalent to:

$$s_i^2 = s_i, \forall i \in N \quad (10)$$

It implies that the main diagonal of matrix \mathbf{S} is equal to \mathbf{s} . Then the binary constraint can be expressed as follows:

$$\text{diag}(\mathbf{S}) = \mathbf{s} \quad (11a)$$

$$\mathbf{S} = \mathbf{ss}^T \quad (11b)$$

Further, it can be proved that (11b) is equivalent to the following [18]:

$$\mathbf{S} \succeq \mathbf{0}, \text{rank}(\mathbf{S}) = 1 \quad (12)$$

Here, $\mathbf{A} \succeq \mathbf{B}$ is meant that matrix $\mathbf{A} - \mathbf{B}$ is positive semidefinite. The first constraint in (12) is linear with respect to variable \mathbf{S} while the rank constraint is not. In fact, the difficulty in **r2** arises from the nonconvexity of the rank constraint. By dropping it, we obtain the following relaxed version of the original quadratic program:

$$\begin{aligned} & \underset{\mathbf{s}, \mathbf{S}}{\text{minimize}} && \langle \mathbf{W}, \mathbf{S} \rangle \\ & \text{subject to} && \text{diag}(\mathbf{S}) = \mathbf{s} \\ & && \mathbf{S} \succeq \mathbf{0} \end{aligned} \quad (13)$$

2) *Relaxation for r2*: Now, we go back to our problem. Define $\mathbf{s} = [s_{l_1}, \dots, s_{l_i}, \dots, s_{l_{|N|}}]^T$ as a $|N| \times 1$ vector and introduce a new matrix $\mathbf{S}^L = \mathbf{ss}^T$. Then the binary constraint in (3f) can be relaxed to:

$$\begin{aligned} & \mathbf{S}_{ii}^L - s_i = 0, \forall i \in N \\ & \mathbf{S}^L \succeq \mathbf{0} \end{aligned} \quad (14)$$

Constraint (3g) can be addressed in a similar manner. We order the transmission lines and define vector $\mathbf{t} = [t^1, \dots, t^i, \dots, t^{|B|}]^T$, where t^i is the circuit breaker's status on i -th transmission line, and $|B|$ is the number of transmission lines in the system. Let matrix variable $\mathbf{S}^t = \mathbf{tt}^T$. Then constraint (3g) can be replaced by:

$$\begin{aligned} & \mathbf{S}_{ii}^t - t_i = 0, i = 1, 2, \dots, |B| \\ & \mathbf{S}^t \succeq \mathbf{0} \end{aligned} \quad (15)$$

Notice that (3f) and (3g) are replaced by (14) and (15) respectively which contain only linear and semidefinite cone constraints. These constraints are known to be convex and are conformed with the formulation of SDP [20]. For now, the only issue left is **r3** (since we have approximated the constraints in **r1**, **r2** with convex ones). As long as we have a tight approximation of probability constraint in (3d) by using linear constraint, the original problem formulation (P1) can be relaxed into a SDP¹. In addition, it is known that several off-the-shelf efficient interior point methods can be used to solve SDPs [21].

¹Please note that all the other constraints are linear.

C. Approximation of Probability Constraint (for r3)

We aim to deal with **r3** in the next step, based on the so-called scenario-based convex approximation [22]. In the first place, (3h) can be rewritten as:

$$\Pr \left\{ P_{L_i} - P_{G_i} - P_{R_i} + \sum_{j \in \mathcal{N}_i} P_{t_{ij}} \leq 0, \forall i \in N \right\} \geq 1 - \epsilon \quad (16)$$

To briefly describe the general scenario-based convex approximation method, consider the prototype probability-constrained problem:

$$\begin{aligned} & \underset{\lambda \in \Lambda}{\text{minimize}} && c^T \lambda \\ & \text{subject to} && \Pr \{ \phi \in \Phi : f(\lambda, \phi) \leq 0 \} \geq 1 - \epsilon \end{aligned} \quad (17)$$

Here λ is the ‘‘design parameter’’ and ϕ denotes the ‘‘uncertainty factor’’ which is a random variable. To be specific, in our problem (in (16)), the set of design parameters $\lambda = \{P_{G_i}, P_{L_i}, P_{t_{ij}}\}$, uncertainty factor $\phi = \{P_{R_i}\}$. In this case, notice that $f(\lambda, \phi) : \Lambda \times \Phi \rightarrow \mathbb{R}^n$ is convex in λ , for any fixed value of $\phi \in \Phi$. Thus, the Assumption 1 in [22] is met. Then (17) can be approximated by the scenario-based approximation method as follows.

$$\begin{aligned} & \underset{\lambda \in \Lambda}{\text{minimize}} && c^T \lambda \\ & \text{subject to} && f(\lambda, \phi^k) \leq 0, k = 1, \dots, M \end{aligned} \quad (18)$$

where $\phi^1, \phi^2, \dots, \phi^M$ are M independently generated samples of ϕ . To apply the scenario-based convex approximation method, we first independently generate M samples $P_{R_i}^1, P_{R_i}^2, \dots, P_{R_i}^M$, and replace the chance-constraint (16) with the linear constraints as follows.

$$P_{L_i} - P_{G_i} - P_{R_i}^k + \sum_{j \in \mathcal{N}_i} P_{t_{ij}} \leq 0, k = 1, \dots, M, \forall i \in N \quad (19)$$

Notice that we select the constraints $f(\lambda, \phi^k) \leq 0$ in a random manner, thus the optimal solution $\hat{\lambda}$ depending on the multi-sample extraction $(\phi^1, \phi^2, \dots, \phi^M)$ is actually a random variable. Therefore, $\hat{\lambda}$ can be a ϵ -level solution for a given random extraction and not for another. Let parameter β bounds the probability that $\hat{\lambda}$ is not a ϵ -level solution (feasible for problem in (17)). Thus, β can be seen as the *risk of failure* associated to the randomized solution algorithm. It is said that if M (specified by the following condition) random scenarios are drawn, the optimal solution in the approximated problem achieves ϵ -level feasibility for the original probability-constrained one with probability no less than $1 - \beta$ [22].

$$M \geq \left\lceil \frac{2}{\epsilon} \ln \frac{1}{\beta} + 2n_\lambda + \frac{2n_\lambda}{\epsilon} \ln \frac{2}{\epsilon} \right\rceil \quad (20)$$

where n_λ is the number of design variables, and $\lceil \cdot \rceil$ denotes the ceil function. Tailoring (20) to our problem, the minimum sample size \hat{M} can be provided based on the proposition as follows.

Proposition 2. Given the power imbalance probability threshold ϵ , and the lower bound

$$M \geq \tilde{M} := \left\lceil \frac{2}{\epsilon} \ln \frac{1}{\beta} + 2(2|N| + |B|) + \frac{2(2|N| + |B|)}{\epsilon} \ln \frac{2}{\epsilon} \right\rceil$$

then the solution to the reformulated problem with constraint (19) is feasible for the original problem with constraint (16), with probability at least as $1 - \beta$.

At this point, a convex-relaxed program of (P2) can be obtained. For simplification, we define:

\mathbf{P}^G	$ N $ -dimensional vector where P_{G_i} is the i -th element.
\mathbf{P}^L	$ N $ -dimensional vector where P_{L_i} is the i -th element.
\mathbf{P}^t	$ B $ -dimensional vector collecting power flows on all lines.
\mathbf{A}	$ N \times B $ oriented incidence matrix of the grid graph.
\mathbf{c}	$ B $ -dimensional vector collects power flow limits on all lines.
\mathbf{C}	$ B \times B $ matrix equals $\text{diag}(\mathbf{c})$.
\mathbf{P}_G^{\min}	$ N $ -dimensional vector where $P_{G_i}^{\min}$ is the i -th element.
\mathbf{P}_G^{\max}	$ N $ -dimensional vector where $P_{G_i}^{\max}$ is the i -th element.
\mathbf{P}_L^{\min}	$ N $ -dimensional vector where $P_{L_i}^{\min}$ is the i -th element.
\mathbf{P}_L^{\max}	$ N $ -dimensional vector where $P_{L_i}^{\max}$ is the i -th element.
$\mathbf{P}_{L_{\min}}$	$ N \times N $ matrix equals $\text{diag}(\mathbf{P}_L^{\min})$.
$\mathbf{P}_{L_{\max}}$	$ N \times N $ matrix equals $\text{diag}(\mathbf{P}_L^{\max})$.
λ_M	$ N $ -dimensional vector where λ_{M_i} is the i -th element.
\mathbf{Q}	$ N $ -dimensional vector where Q_i is the i -th entry.
\mathbf{P}_R^k	$ N $ -dimensional vector where $P_{R_i}^k$ is the i -th entry.

Now we can express our computationally tractable reformulation as follows.

$$(P3) \quad \underset{\mathcal{D}}{\text{minimize}} \quad \begin{bmatrix} t_1, t_2 \end{bmatrix}^T \quad (21a)$$

$$\text{subject to:} \quad (14) - (15) \text{ and} \quad (21b)$$

$$-\mathbf{c} \preceq \mathbf{P}^t \preceq \mathbf{c} \quad (21c)$$

$$-\mathbf{C}\mathbf{t} \preceq \mathbf{P}^t \preceq \mathbf{C}\mathbf{t} \quad (21d)$$

$$\mathbf{P}_G^{\min} \preceq \mathbf{P}^G \preceq \mathbf{P}_G^{\max} \quad (21e)$$

$$\mathbf{P}_{L_{\min}}\mathbf{s} \preceq \mathbf{P}^L \preceq \mathbf{P}_{L_{\max}}\mathbf{s} \quad (21f)$$

$$\lambda_M^T \mathbf{Q} \geq -t_1 \quad (21g)$$

$$\mathbf{0} \preceq \mathbf{Q} \preceq \mathbf{P}^L \quad (21h)$$

$$\mathbf{P}^L + \mathbf{P}_{L_{\max}}\mathbf{s} - \mathbf{P}_L^{\max} \preceq \mathbf{Q} \preceq \mathbf{P}_{L_{\max}}\mathbf{s} \quad (21i)$$

$$-\mathbf{c} - t_2\mathbf{1}^T \preceq \mathbf{P}^t \preceq \mathbf{c} + t_2\mathbf{1}^T \quad (21j)$$

$$\mathbf{P}^L - \mathbf{P}_R^k - \mathbf{P}^G + \mathbf{A}\mathbf{P}^t \preceq \mathbf{0}, \quad k = 1, \dots, M \quad (21k)$$

where $\mathcal{D} := \{\mathbf{P}^G, \mathbf{P}^L, \mathbf{P}^t, \mathbf{Q}, \mathbf{t}, \mathbf{s}, \mathbf{S}^L, \mathbf{S}^t, t_1, t_2\}$ contains all the decision variables (for convenience, “ \preceq ” is a component-wise operator in 21b-21k). For a practical use, (21k) can be replaced by the following to reduce the number of constraints.

$$\mathbf{P}^L - \mathbf{P}^G + \mathbf{A}\mathbf{P}^t \preceq \min_{k=1, \dots, M} \mathbf{P}_R^k \quad (22)$$

where $\min_{k=1, \dots, M} \mathbf{P}_R^k$ is the vector that its i -th element corresponds to the minimum value of P_{R_i} among the M samples. Note that (P3) is a SDP relaxed reformulation for our proposed

microgrid reconfiguration. To solve (P3), a weighted-sum method based scheme is presented next.

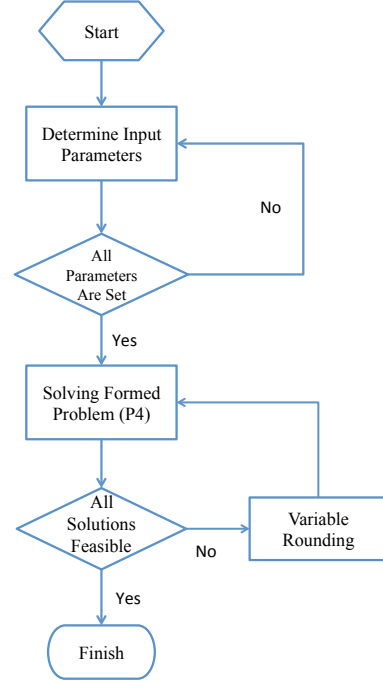


Fig. 3. Flowchart of the Solution Methodology

V. MULTI-OBJECTIVE OPTIMIZATION AND ROUNDING MECHANISM

Multi-objective programming is concerned with optimization problems seeking to optimize more than one objective function simultaneously. A general form is casted as follows.

$$\begin{aligned} &\text{minimize} \quad \mathbf{C}(\mathbf{u}) = [c_1(\mathbf{u}), c_2(\mathbf{u}), \dots, c_m(\mathbf{u})]^T \\ &\text{subject to:} \quad \mathbf{u} \in \Omega \end{aligned} \quad (23)$$

where $\Omega = \{\mathbf{u} \in \mathbb{R}^n : f(\mathbf{u}) \leq 0, l(\mathbf{u}) = 0\}$ denotes the feasible solution region. $c_i(\mathbf{u})$ represents the i -th objective, \mathbf{u} is the unknown variable, m is the number of the objectives, and $f(\mathbf{u})$ and $l(\mathbf{u})$ account for the involving constraints (inequality and equality) in the problem. Note that, the objectives in the problem have tradeoffs among them (otherwise it becomes a single-objective program), thus no unique best decision exists. Specifically, the so-called *Pareto optimal solution* is used to represent the set of “optimal” solutions of the multi-objective problem. A formal definition is introduced below.

Pareto optimal solution: A feasible solution \mathbf{u}^* of the optimization program (23) with no any another feasible solution $\mathbf{u} \in \Omega$ satisfying $c_i(\mathbf{u}) \geq c_i(\mathbf{u}^*)$ for every index i , and for at least an index j that $c_j(\mathbf{u}) > c_j(\mathbf{u}^*)$.

A. Solving the multi-objective problem (P3)

We used the weighted-sum method in this paper to solve (P3). It naturally transforms the vector of objectives into a

scalar form, which can be posed as follows.

$$\begin{aligned} & \underset{\mathbf{u} \in \Omega}{\text{minimize}} && \sum_{i=1}^m w_i c'_i(\mathbf{u}) \\ & \text{subject to} && \sum_{i=1}^m w_i = 1, \quad w_i \geq 0, \quad i = 1, 2, \dots, m \end{aligned} \quad (24)$$

where w_i denotes the preference of the i -th objective, and $c'_i(\mathbf{u})$ is the normalized version of objective function $c_i(\mathbf{u})$. It has been proved that if $c_i(\mathbf{u}), i = 1, 2, \dots, m$ and Ω are all convex, then applying the weighted-sum method in (24) can generate any Pareto solution of (23) [23].

Based on the facts above, the optimization problem (P3) can be converted in an alternative way as follows.

$$\begin{aligned} \text{(P4)} \quad & \underset{\mathcal{D}}{\text{minimize}} && \frac{w_1}{N_1} t_1 + \frac{w_2}{N_2} t_2 \\ & \text{subject to:} && (21\text{b}) - (21\text{k}) \text{ and} \\ & && w_1 + w_2 = 1, \quad w_1, w_2 \geq 0 \end{aligned}$$

where N_1, N_2 are the known normalization factors of objectives t_1 and t_2 respectively.

We see that (P4) is our final SDP-based microgrid reconfiguration formulation. However, in the results of (P4), the binary variables \mathbf{s}^* and \mathbf{t}^* denoting the status of the circuit breaks might have values between 0 and 1. Thus the next step is to convert these solutions to obtain the valid Boolean status, often referred to as ‘‘rounding’’.

B. Variable Threshold Rounding

Regard \mathbf{s}^* and \mathbf{t}^* as the values of \mathbf{s} and \mathbf{t} in the optimal solution of (P4) respectively. Let \mathbf{s}^r and \mathbf{t}^r represent the solutions after rounding. Then we adopt a simple rounding mechanism as follows.

We drop the obtained matrices $(\mathbf{S}^L)^*$ and $(\mathbf{S}^t)^*$, keeping only the vectors \mathbf{s}^* and \mathbf{t}^* , and round their elements to 0 or 1. It is stated as:

$$\begin{aligned} \mathbf{s}_i^r &= \text{sign}(\mathbf{s}^* - \mu), \quad i = 1, 2, \dots, |N| \\ \mathbf{t}_i^r &= \text{sign}(\mathbf{t}^* - \mu), \quad i = 1, 2, \dots, |B| \end{aligned} \quad (25)$$

where $\mu \in (0, 1)$ is a predefined threshold and the function sign is:

$$\text{sign}(y) = \begin{cases} +1, & y \geq 0; \\ -1, & y < 0. \end{cases} \quad (26)$$

After the rounding process for the breakers status variables \mathbf{s} and \mathbf{t} , we can plug them into (P4) and run the optimization again to obtain the rest of the decision variables in \mathcal{D} .

VI. PRELIMINARY NUMERICAL TESTS

In this section, a modified 7-node test feeder (shown in Fig. 4) [13] was considered to study the performance and properties of the proposed approach. The grid reconfiguration problem formulated in (P4) was solved by the package CVX ([24]) in MATLAB. The power imbalance probability is set to $\epsilon = 0.01(1\%)$, and the parameter β in proposition 2 is 0.05. According to proposition 2, approximately at least 2183

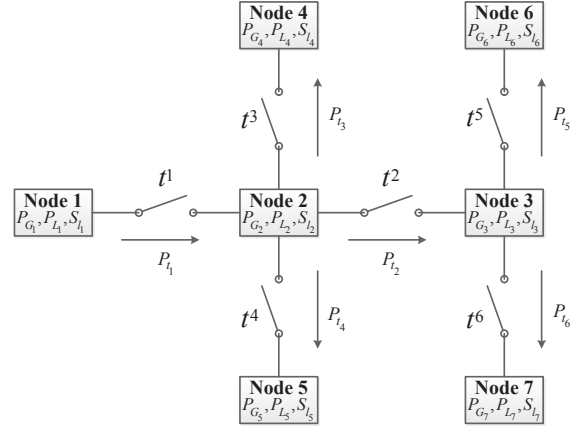


Fig. 4. Example of 7-node Test Feeder

TABLE II
PARAMETER SETTING OF 7-NODE TEST FEEDER (INITIAL CASE)

Parameter	Initial Setting
\mathbf{c}	$[2, 2, 2, 2, 2, 2]^T$ (kW)
\mathbf{P}_G^{\min}	$[0, 0, 0, 0, 0, 0]^T$ (kW)
\mathbf{P}_G^{\max}	$[1, 0, 2, 6, 6, 6]^T$ (kW)
\mathbf{P}_L^{\min}	$[2, 2, 2, 2, 2, 2]^T$ (kW)
\mathbf{P}_L^{\max}	$[5, 5, 5, 5, 5, 5]^T$ (kW)
λ_M	$[1, 0.8, 0.7, 0.6, 0.5, 0.2, 0.1]^T$

samples are required. In this study, we used 5000 samples of renewable energy generation for each P_{R_i} at i -th node. The renewable energy generation P_{R_i} is modeled as a Gaussian distributed random variable for each node i following distribution $\mathcal{N}(2, 0.2)$. The threshold μ is set to 0.6. The matrix \mathbf{A} can be formed based on the connectivity topology in Fig. 4. The other parameter settings are illustrated in the ensuing context. We first study an initial case with the parameter setting in TABLE II. Fig. 5 shows the pareto points generated from the solution of (P4). The average number of iterations for the interior-point solver of CVX were 20 and the computation time was 1.2 seconds on a machine with Intel Duo Core 1.8GHZ. For the system operator, if the objective of total loads served has higher preference than the reconfiguration operation reliability, then the points around the right lower corner of Fig. 5 might be good choices. In contrast, if the operation reliability is seen more important than the total loads served, then the points around the left upper corner become right options.

TABLE III-IV illustrate the best solutions obtained by SDP approach for minimizing the negative of total loads served (t_1) and the negative of reconfiguration operation reliability (t_2), respectively under the initial setting case. From TABLE III-IV, it can be observed that the tradeoff between objectives of total loads served and reconfiguration reliability do exist. In particular, the value of t_2 in TABLE III is extremely close to zero, which means at least one branch almost reaches its power flow limit. This verifies our concern that if only the

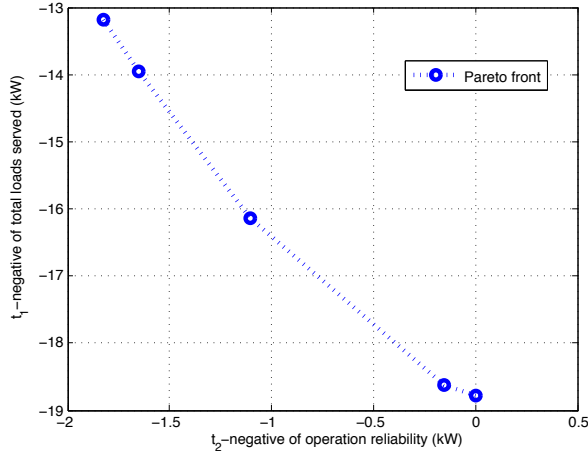


Fig. 5. Pareto points of reconfiguration problem with initial setting

TABLE III

BEST SOLUTION FOR THE NEGATIVE OF TOTAL LOADS SERVED

Results	Min. t_1
\mathbf{P}^G	$[1.00, 0.00, 1.79, 5.79, 5.80, 5.49, 5.47]^T$
\mathbf{P}^L	$[4.27, 5.00, 5.00, 5.00, 5.00, 5.00, 5.00]^T$
\mathbf{P}^t	$[-2.00, -1.92, -1.90, -1.90, -1.12, -1.13]^T$
$[t_1, t_2]$	$[-18.77, 1.02\text{E-}08]^T$

TABLE IV

BEST SOLUTION FOR THE NEGATIVE OF RECONFIGURATION RELIABILITY

Results	Min. t_2
\mathbf{P}^G	$[1.00, 0.00, 2.00, 5.12, 5.12, 5.15, 5.14]^T$
\mathbf{P}^L	$[2.10, 2.00, 3.55, 5.00, 5.00, 5.00, 5.00]^T$
\mathbf{P}^t	$[0.17, -0.17, -0.17, -0.17, -0.17, -0.17]^T$
$[t_1, t_2]$	$[-13.19, -1.83]^T$

objective of total loads served is considered, the power flows in branches might reach their limits which will significantly increase the risk of power-line fault/outage.

A. The effect of changing parameter \mathbf{P}_G^{\max}

For investigating the impact of variation of parameter \mathbf{P}_G^{\max} on the pareto points, we consider the second test case. We use the same parameters as in the initial case except that $\mathbf{P}_G^{\max} = [1, 0, 2, 4, 4, 4, 4]^T$. The resulting solution is depicted in Fig. 6. We find that the value of t_1 in the right lower extreme point is higher than its counterpart in Fig. 5. It implies that the best solution for total loads served in case 2 is inferior to the best solution in the initial case. This phenomenon can be expected since the parameters of maximum power generations of DGs in node 4 – 7 have been reduced in case 2.

B. The effect of changing parameter \mathbf{P}_L^{\min}

Fig. 7 illustrates the pareto optimal points obtained through various values of vector \mathbf{P}_L^{\min} . Lmin=1.5 means the minimum load required for each node is 1.5 kW (every component of

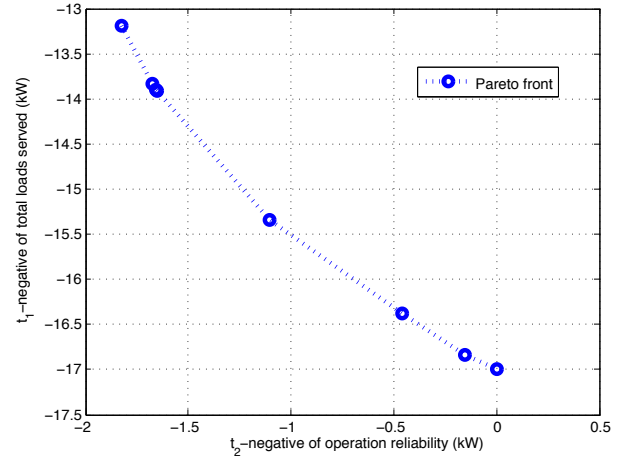


Fig. 6. Pareto points of reconfiguration problem (case 2)

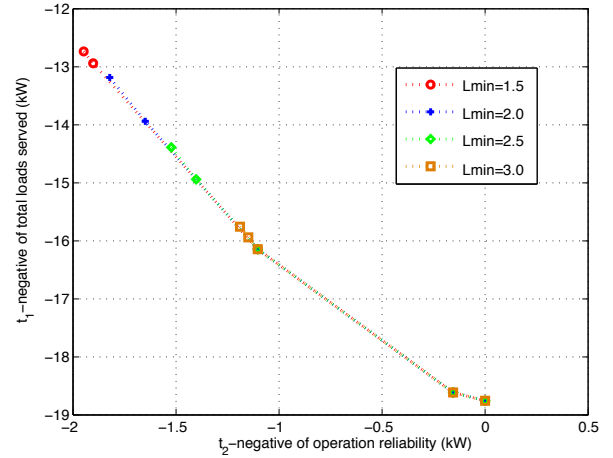


Fig. 7. Comparison of Pareto points with different values of \mathbf{P}_L^{\min}

\mathbf{P}_L^{\min} equals 1.5). We first note that the generated points belong to a same pareto front. This is because in these scenarios, the amount of minimum loads required is relatively small comparing to the power generations. For each node, the “actual” load supplied can always be greater than the minimum limit (Lmin=3.0). Thus, cases with Lmin=2.0, 2.5, 3.0 are within the solution set of Lmin=1.5. Fig. 7 also implies that when each node wants more energy for its minimum consumption, the reconfiguration operation would be less reliable.

Another thing can be expected is that, for example, if node 1 and node 2 do not have enough generations to satisfy their own minimum loads and the lines connecting node 1 and node 2 with the rest of the network do not have enough capacity to transmit power for satisfying at least their minimum loads, these two nodes might isolate themselves from the network². Due to space limitation, we omit the detailed results on this scenario.

²The breakers status are all obtained to be closed in this paper.

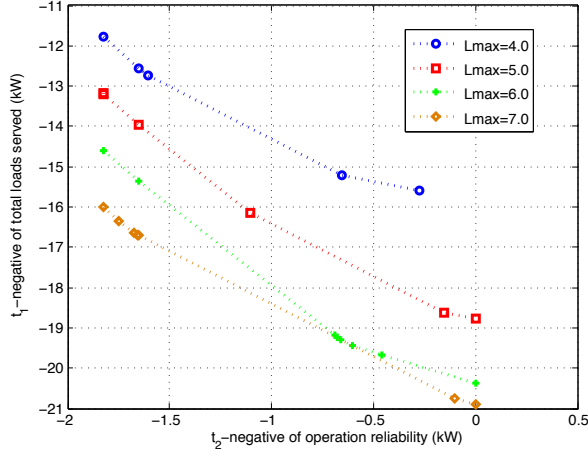


Fig. 8. Comparison of Pareto fronts with different values of \mathbf{P}_L^{\max}

C. The effect of changing parameter \mathbf{P}_L^{\max}

In a similar way as section VI-B, we perform tests on different values of vector \mathbf{P}_L^{\max} . In Fig. 8, we notice that with larger value of maximum load needed for each node, the pareto front is lower. We observe that if the system can supply at least some nodes with their maximum loads wanted (most satisfied situation for the nodes), the total objective value with larger Lmax is superior to its counterpart with smaller one.

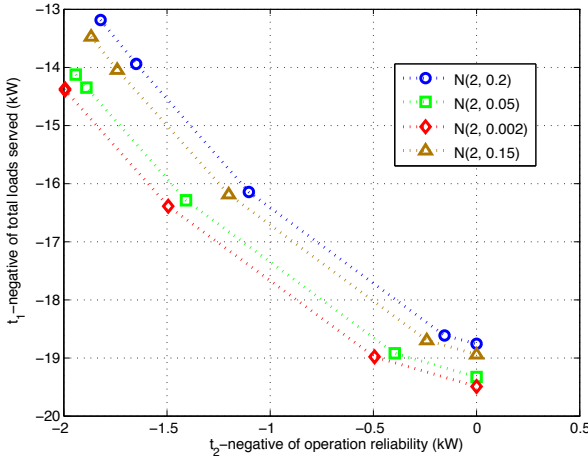


Fig. 9. Comparison of Pareto fronts with different variances of RES generation

D. The effect of RES generation uncertainty

We also study the effect of RES generation uncertainty on the Pareto front. The variances of the renewable energy generation P_{R_i} for each node i are set to 0.2, 0.15, 0.05, 0.002 (the mean value is kept the same). The other settings are the same as the initial case in TABLE II. The simulated results in Fig. 9 show that larger variance of RES generation results in less efficient reconfiguration operation. The reason for that might be as follows. If the variance of RES generation is large, the optimal operation would be “conservative” to

use RES (since the algorithm is “very unsure” on the RES generation and its amount might be underestimated), which will decrease the total efficiency. Nevertheless, the proposed algorithm would rather sacrifice the efficiency to reduce the probability of power imbalance.

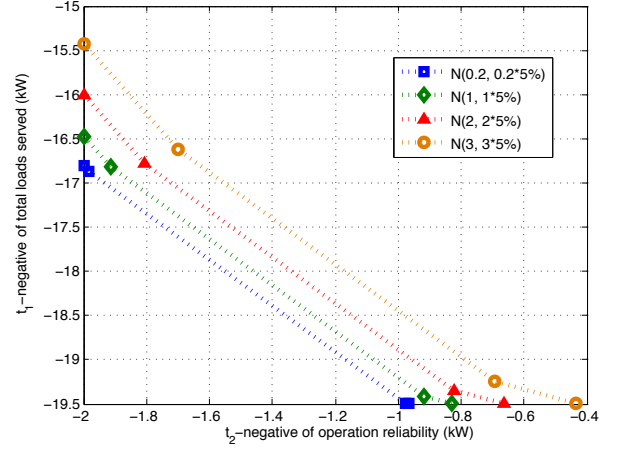


Fig. 10. Comparison of Pareto fronts with various levels of RES penetration

E. The level of RES penetration in total power generation

In this section, we assess the effect of changing the level of RES penetration in each node. To this end, we fixed the maximum power generation capacities of the 7 nodes to [4, 3, 5, 7, 7, 7, 7], respectively. The statistical means of RES generation are set to 0.2, 1, 2, 3, and the maximum conventional DG generation vector \mathbf{P}_G^{\max} is changed accordingly. The variances are set to 5% of their means. As shown in Fig. 10, an interesting fact is that as the level of RES penetration grows, the efficiency measured by the total objectives decreases. In other words, in these reliability-concerned microgrid restoration problems, the proposed algorithm might prefer more “reliable” power sources (i.e. conventional DG) to RES.

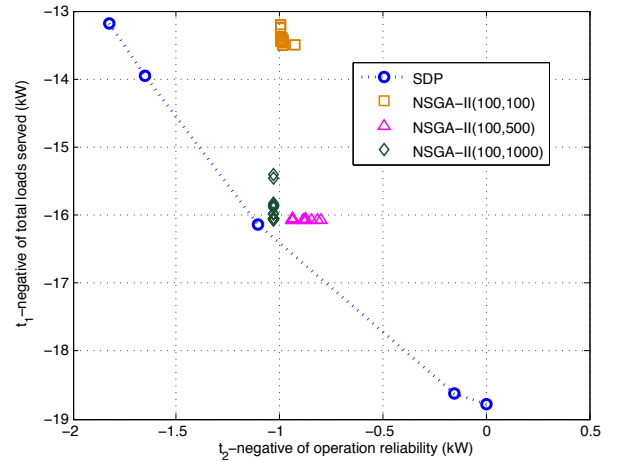


Fig. 11. Comparison of Pareto points of the SDP-based method and NSGA-II

F. Comparison of the SDP-based method and NSGA-II

Finally, in Fig. 11, we do compare our proposed SDP-based approach with a widely used multi-objective evolutionary algorithm, called Nondominated Sorting Genetic Algorithm II (NSGA-II) [25] on the initial case (described in TABLE II). We test NSGA-II with population size 100 and obtain the pareto fronts at generation 100, 500, and 1000 respectively. It is observed in Fig. 11 that the SDP-based method generate slightly less number of solutions than NSGA-II. Nevertheless, our proposed method has better solutions in general (also reaches two extreme points). And it avoids the problem of the clustering of the solution points appearing in NSGA-II.

VII. CONCLUSION

A novel multi-objective microgrid reconfiguration scheme was proposed in this paper. To overcome the difficulties in solving the resultant optimization problem, the convex relaxation techniques and the scenario approximation approach were adopted to obtain a computationally tractable SDP reformulation. The generated Pareto-optimal points from the SDP reformulation in various tests illustrated its correctness and meliority in providing critical planning information to system decision-makers. Studying the proposed scheme on more complicating and practical microgrid power networks are currently under investigation.

REFERENCES

- [1] N. Hatziaargyriou, H. Asano, R. Iravani, and C. Marnay, "Microgrids," *IEEE Power and Energy Magazine*, vol. 5, no. 4, pp. 78–94, July 2007.
- [2] S. Karnouskos, "Cyber-physical systems in the smartgrid," in *Industrial Informatics (INDIN), 2011 9th IEEE International Conference on*, July 2011, pp. 20–23.
- [3] R. Brown, "Impact of smart grid on distribution system design," in *Power and Energy Society General Meeting - Conversion and Delivery of Electrical Energy in the 21st Century, 2008 IEEE*, July 2008, pp. 1–4.
- [4] A. Tsikalakis, Y. Katsigiannis, P. Georgilakis, and N. Hatziaargyriou, "Determining and exploiting the distribution function of wind power forecasting error for the economic operation of autonomous power systems," in *IEEE Power Engineering Society General Meeting*, 2006, pp. 1–8.
- [5] P. Bacher, H. Madsen, and H. A. Nielsen, "Online short-term solar power forecasting," *Solar Energy*, vol. 83, no. 10, pp. 1772–1783, 2009. [Online]. Available: <http://www.sciencedirect.com/science/article/pii/S0038092X09001364>
- [6] R. S. Rao, S. V. L. Narasimham, and M. Ramalingaraju, "Optimization of distribution network configuration for loss reduction using artificial bee colony algorithm," *International Journal of Electrical Power and Energy Systems Engineering*, pp. 116–122, 2008.
- [7] A. Abdelaziz, F. Mohamed, S. Mekhamer, and M. Badr, "Distribution system reconfiguration using a modified tabu search algorithm," *Electric Power Systems Research*, vol. 80, no. 8, pp. 943–953, 2010. [Online]. Available: <http://www.sciencedirect.com/science/article/pii/S037877961000012X>
- [8] K. S. Kumar and T. Jayabarathi, "Power system reconfiguration and loss minimization for a distribution systems using bacterial foraging optimization algorithm," *International Journal of Electrical Power and Energy Systems*, vol. 36, no. 1, pp. 13–17, 2012. [Online]. Available: <http://www.sciencedirect.com/science/article/pii/S0142061511002651>
- [9] H. Khodr, J. Martinez-Crespo, M. Matos, and J. Pereira, "Distribution systems reconfiguration based on opf using benders decomposition," *IEEE Transactions on Power Delivery*, vol. 24, no. 4, pp. 2166–2176, Oct 2009.
- [10] D. Das, "A fuzzy multiobjective approach for network reconfiguration of distribution systems," *IEEE Transactions on Power Delivery*, vol. 21, no. 1, pp. 202–209, Jan 2006.
- [11] S. R. S. N. Shanmuga Vadivoo, "Distribution system restoration using genetic algorithm with distributed generation," *Modern Applied Science*, 2009.
- [12] S. Bose, S. Pal, B. Natarajan, C. Scoglio, S. Das, and N. Schulz, "Analysis of optimal reconfiguration of shipboard power systems," *IEEE Transactions on Power Systems*, vol. 27, no. 1, pp. 189–197, Feb 2012.
- [13] S. Gupta, W. Yeoh, E. Pontelli, P. Jain, and S. Ranade, "Modeling microgrid islanding problems as dcops," in *North American Power Symposium (NAPS)*, Sept 2013, pp. 1–6.
- [14] R. M. Vitorino, H. M. Jorge, and L. P. Neves, "Multi-objective optimization using nsga-ii for power distribution system reconfiguration," *International Transactions on Electrical Energy Systems*. [Online]. Available: <http://dx.doi.org/10.1002/etep.1819>
- [15] M. Fukuda and M. Kojima, "Branch-and-cut algorithms for the bilinear matrix inequality eigenvalue problem," *Comput. Optim. Appl.*, vol. 19, no. 1, pp. 79–105, Apr. 2001. [Online]. Available: <http://dx.doi.org/10.1023/A:1011224403708>
- [16] O. Toker and H. Ozbay, "On the np-hardness of solving bilinear matrix inequalities and simultaneous stabilization with static output feedback," in *American Control Conference, Proceedings of the 1995*, vol. 4, Jun 1995, pp. 2525–2526.
- [17] Y. Nesterov and A. Nemirovskii, *Interior Point Polynomial Algorithms in Convex Programming*, ser. Studies in Applied Mathematics. Society for Industrial and Applied Mathematics, 1994. [Online]. Available: <http://books.google.com/books?id=C-MjQ98V9e0C>
- [18] Z.-Q. Luo, W.-K. Ma, A.-C. So, Y. Ye, and S. Zhang, "Semidefinite relaxation of quadratic optimization problems," *IEEE Signal Processing Magazine*, vol. 27, no. 3, pp. 20–34, 2010.
- [19] F. Barahona, M. Junger, and G. Reinelt, "Experiments in quadratic 0-1 programming," *Math. Program.*, vol. 44, no. 2, pp. 127–137, Jul. 1989. [Online]. Available: <http://dx.doi.org/10.1007/BF01587084>
- [20] S. Boyd and L. Vandenberghe, *Convex Optimization*. New York, NY, USA: Cambridge University Press, 2004.
- [21] A. S. Nemirovski and M. J. Todd, "Interior-point methods for optimization," *Acta Numerica*, pp. 191–234, 2008.
- [22] G. Calafiore and M. Campi, "The scenario approach to robust control design," *IEEE Transactions on Automatic Control*, vol. 51, no. 5, pp. 742–753, May 2006.
- [23] K. Miettinen, *Nonlinear multiobjective optimization*. Kluwer Academic Publishers, Boston, 1999.
- [24] M. Grant and S. Boyd, "CVX: Matlab software for disciplined convex programming, version 2.0 beta," <http://cvxr.com/cvx>, Sep. 2013.
- [25] K. Deb, A. Pratap, S. Agarwal, and T. Meyarivan, "A fast and elitist multiobjective genetic algorithm: Nsga-ii," *IEEE Transactions on Evolutionary Computation*, vol. 6, no. 2, pp. 182–197, Apr 2002.